Journal of Engineering Mechanics ASCE , Vol. 134 (2008), in press

What Did and Did not Cause Collapse of WTC Twin Towers in New York

Zdeněk P. Bažant, Jia-Liang Le, Frank R. Greening and David B. Benson

Structural Engineering Report No. 07-05/C605c

Department of Civil and Environmental Engineering
Northwestern University
Evanston, Illinois 60208, USA

May 27, 2007
Revised June 22, December 15, 2007, and March 31, 2008

What Did and Did Not Cause Collapse of WTC Twin Towers in New York

Zdeněk P. Bažant[1], Hon.M. ASCE, Jia-Liang Le[2], Frank R. Greening[3], and David B. Benson[4]

Abstract: Previous analysis of progressive collapse showed that gravity alone suffices to explain the overall collapse of the World Trade Center (WTC) towers. However, it remains to be checked whether the recent allegations of controlled demolition have any scientific merit. The present analysis proves that they do not. The video record available for the first few seconds of collapse is shown to agree with the motion history calculated from the differential equation of progressive collapse but, despite uncertain values of some parameters, it is totally out of range of the free fall hypothesis, on which these allegations rest. It is shown that the observed size range (0.01 mm—0.1 mm) of the dust particles of pulverized concrete is consistent with the theory of comminution caused by impact, and that less than 10% of the total gravitational energy, converted to kinetic energy, sufficed to produce this dust (whereas more than 150 tons of TNT per tower would have to be installed, into many small holes drilled into concrete, to produce the same pulverization). The air ejected from the building by gravitational collapse must have attained, near the ground, the speed of almost 500 mph (or 223 m/s, or 803 km/h) on the average, and fluctuations must have reached the speed of sound. This explains the loud booms and wide spreading of pulverized concrete and other fragments, and shows that the lower margin of the dust cloud could not have coincided with the crushing front. The resisting upward forces due to pulverization and to ejection of air, dust and solid fragments, neglected in previous studies, are found to be indeed negligible during the first few seconds of collapse but not insignificant near the end of crush-down. The calculated crush-down duration is found to match a logical interpretation of seismic record, while the free fall duration grossly disagrees with this record.

Introduction

To structural engineers, the collapse of the World Trade Center (WTC) towers on 9/11/2001 came as the greatest surprise since the collapse of Tacoma Narrows Bridge in 1940. Immediately after the aircraft impact, the structural frame behaved as expected, but not after the fire.

To explain the collapse, it was proposed (on September 13, 2001; Bažant 2001; Bažant and Zhou 2002) that viscoplastic buckling of heated and overloaded columns caused the top part of tower to fall through the height of at least one story, and then shown that the kinetic energy of the impact on the lower part must have exceeded the energy absorption capacity of the lower part by an order of magnitude. A meticulous investigation of unprecedented scope and detail, conducted by S. Shyam Sunder's team at the National Institute of Standards and Technology (NIST 2005), supports this explanation. Although NIST did not analyze the overall process of dynamic progressive collapse below the fire zone, it verified a sequence of effects that triggered the collapse: (1) scraping of much of steel insulation by flying objects during aircraft impact (without which the towers would not have collapsed, as concluded by NIST); (2) cutting of many columns, and damage with large deflections of others during aircraft impact; (3) subsequent load redistributions among columns; (4) sagging of heated floor trusses and their catenary action, evidenced by multistory inward bowing of perimeter columns; and (5) viscoplastic buckling of heated, damaged and overloaded columns.

Universally though has the foregoing explanation of collapse been accepted by the communities of structural engineers and structural mechanics researchers, some outside critics have nevertheless exploited various unexplained observations to disseminate allegations of controlled demolition. The objective of this paper, based on the report by Bažant et al. (2007), is to examine whether those allegations might be scientifically justifiable, and to show that the concept of gravity-driven collapse does not conflict with any observations.

[1]McCormick Institute Professor and W.P. Murphy Professor of Civil Engineering and Materials Science, Northwestern University, 2145 Sheridan Road, CEE/A135, Evanston, Illinois 60208; z-bazant@northwestern.edu.

[2]Graduate Research Assistant, Northwestern University.

[3]Engineering Consultant, Hamilton, Ontario L8S 3X7.

[4]Professor Emeritus, School of Electrical Engrg. and Computer Science, Washington State University, Pullman, WA 99164.

NIST examined paint cracking on 16 perimeter columns and only 3 of them showed evidence of temperature $> 250°$C. From annealing studies, the microstructures of recovered steel samples show no evidence of exposure to temperature above 600° C for any significant time (NIST 2005, part NCSTAR 1-3, p.132) (i.e., $>$ 15 min.). Nevertheless, evidence of very high temperature (around 800° C) was found in one unidentified steel column, though it is unlikely that this column was located in the fire stories and experienced high temperature prior to the collapse (NIST 2005, part NCSTAR 1-3C p. 229). Note, though, that only 1% of the columns from the fire stories were examined. Consequently, NIST cautioned that the findings from paint cracking test and annealing studies are not indicative of the steel temperature in the fire stories. Thus, although very high steel temperature are likely, there is no direct evidence. But are high steel temperatures really necessary to explain collapse?

Not really. The initial speculation that very high temperatures were necessary to explain collapse must be now revised since tests revealed a strong temperature effect on the yield strength of the steel used. The tests by NIST (2005, part NCSTAR 1-3D, p. 135, Fig. 6-6) showed that, at temperatures 150°C, 250°C and 350°C, the yield strength of the steel used in the fire stories decreased by 12%, 19% and 25%, respectively. These reductions apply to normal durations of laboratory strength tests (up to several minutes). Since the thermally activated decrease of yield stress is a time-dependent process, the yield strength decrease must have been even greater for the heating durations in the towers, which were of the order of one hour. These effects of heating are further documented by the recent fire tests of Zeng et al. (2003), which showed that structural steel columns under a sustained load of 50% to 70% of their cold strength collapse when heated to 250°C.

Although a detailed computer analysis of columns stresses after aircraft impact is certainly possible, it would be quite tedious and demanding, and has not been carried out by NIST. Nevertheless, it can easily be explained that the stress in some surviving columns most likely exceeded 88% of their cold strength σ_0. In that case, any steel temperature $\geq 150°$C sufficed to trigger the viscoplastic buckling of columns (Bažant and Le 2008). This conclusion is further supported by simple calculations showing that if, for instance, the column load is raised at temperature 250°C from $0.3P_t$ to $0.9P_t$ (where P_t = failure load = tangent modulus load), the critical time of creep buckling (Bažant and Cedolin 2003, chapters 8 and 9) gets shortened from 2400 hours to 1 hour (note that, in structural mechanics, the term 'creep buckling' or 'viscoplastic buckling' represents any time-dependent buckling; on the other hand, in materials science, the term 'creep' is reserved for the time-dependent deformation at stresses $< 0.5\sigma_0$, while the time-dependent deformation at stresses near σ_0 is called the 'flow'; Frost and Ashby 1982).

Therefore, to decide whether the gravity-driven progressive collapse is the correct explanation, the temperature level alone is irrelevant (Bažant and Le 2008). It is meaningless and a waste of time to argue about it without calculating the stresses in columns. For low stress, high temperature is necessary to cause collapse, but for high enough stress, even a modestly elevated temperature will cause it.

The fact that, after aircraft impact, the loads of some columns must have been close to their strength limit can be clarified by Fig. 1. The asymmetry of aircraft impact damage caused the stiffness centroid of the story to acquire a significant eccentricity, e (Fig. 1b). The corresponding bending moment Pe of gravity load $P = m_0 g$ (m_0 = mass of the initial upper falling part; and g = gravity acceleration) caused nonuniform axial shortening and axial stresses in the surviving columns (Fig. 1e,h), which raised the stresses in the columns on the weaker side of story much above the average stress due to gravity. The subsequent heating weakened the overloaded columns on the weaker side (left side in the figure) more than those on the stronger side, and caused gradually more and more of them to lose their load-carrying capability. This further enlarged e and thus increased the nonuniformity of column deformations and stresses (Fig. 1f,i), until the buckling of a sufficient number of columns led to the overall stability loss.

The observed multistory inward bowing of some perimeter columns (Fig. 1c), which reached 1.40 m, must have been a significant factor in stability loss, since the tripling of buckling length reduces the column capacity 9-times. As noted by NIST, the bowing must have been caused by sagging of heated floor trusses, due to their viscoplastic deformation (however, as pointed out by Bažant and Le 2008, the differential thermal expansion could not have been the main cause of bowing since a temperature difference of above 1000°C across the floor truss would be needed to cause a curvature for which the truss span gets shortened by 1.40 m).

Inabsorbable Kinetic Energy

First, let us review the basic argument (Bažant 2001; Bažant and Zhou 2002). After a drop through at least the height h of one story heated by fire (stage 3 in Fig. 2 top), the mass of the upper part of each tower has lost enormous gravitational energy, equal to m_0gh. Because the energy dissipation by buckling of the hot columns must have been negligible by comparison, most of this energy must have been converted into kinetic energy $\mathcal{K} = m_0v^2/2$ of the upper part of tower, moving at velocity v. Calculation of energy W_c dissipated by the crushing of all columns of the underlying (cold and intact) story showed that, approximately, the kinetic energy of impact $\mathcal{K} > 8.4\, W_c$ (Eq. 3 of Bažant and Zhou 2002).

It is well known that, in inelastic buckling, the deformation must localize into inelastic hinges (Bažant and Cedolin 2003, sec. 7.10). To obtain an upper bound on W_c, the local buckling of flanges and webs, as well as possible steel fracture, was neglected (which means that the ratio $\mathcal{K}/W_c$ was at least 8.4). When the subsequent stories are getting crushed, the loss m_0gh of gravitational energy per story exceeds W_c exceeds 8.4 by an ever increasing margin, and so the velocity v of the upper part must increase from one story to the next. This is the basic characteristic of progressive collapse, well known from many previous disasters with causes other than fire (internal or external explosions, earthquake, lapses in quality control; see, e.g., Levy and Salvadori 1992; Bažant and Verdure 2007).

Merely to get convinced of the inevitability of gravity driven progressive collapse, further analysis is, for a structural engineer, superfluous. Further analysis is nevertheless needed to dispel false myths, and also to acquire full understanding that would allow assessing the danger of progressive collapse in other situations.

Generalization of Differential Equation of Progressive Collapse

The gravity-driven progressive collapse of a tower consists of two phases—the crush-down, followed by crush-up (Fig. 2 bottom), each of which is governed by a different differential equation (Bažant and Verdure 2007, pp. 312-313). During the crush-down, the falling upper part of tower (C in Fig. 2 bottom), having a compacted layer of debris at its bottom (zone B), is crushing the lower part (zone A) with negligible damage to itself. During the crush-up, the moving upper part C of tower is being crushed at bottom by the compacted debris B resting on the ground.

The fact that the crush-up of entire stories cannot occur simultaneously with the crush-down is demonstrated by the condition of dynamic equilibrium of compacted layer B, along with an estimate of the inertia force of this layer due to vertical deceleration or acceleration; see Eq. 10 and Fig. 2(f) of Bažant and Verdure (2007). This previous demonstration, however, was only approximate since it did not take into account the variation of crushing forces F_c and F_c' during the collapse of a story. An accurate analysis of simultaneous (deterministic) crush-up and crush-down is reported in Bažant and Le (2008) and is reviewed in the Appendix, where the differential equations and the initial conditions for a two-way crush are formulated. It is found that, immediately after the first critical story collapses, crush fronts will propagate both downwards and upwards. However, the crush-up front will advance into the overlying story only by about 1% of its original height h and then stop. Consequently, the effect of the initial two-way crush is imperceptible and the hypothesis that the crush-down and crush-up cannot occur simultaneously is almost exact.

The aforementioned distance of initial crush-up would be larger if the column cross sections changed discontinuously right below or right above the first collapsed story. However, this does not appear to be the case. A sudden change of column cross section after the crush-down front has advanced by more than a few stories would not produce crush-up because the compacted layer B has already become quite massive and acquired a significant kinetic energy.

As an improvement over previous studies, we take into account the fact that a variation of the initial mass density of stories causes the compaction ratio $\lambda(z)$ to be variable. Consequently, the distribution of velocity $v(z)$ throughout the compacted layer B in the crush-down phase is non-uniform. The equation of motion for the upper part of tower (parts C and B together) during crush-down may be written as

$$\frac{\mathrm{d}}{\mathrm{d}t}\left\{\int_0^{z(t)} \mu(S)\dot{s}(S)\mathrm{d}S\right\} - g\int_0^{z(t)} \mu(S)\mathrm{d}S = -F_c(z,\dot{z}) \tag{1}$$

where t = time, z = vertical (Lagrangian) coordinate = distance of the current crushing front from the initial position of the tower top; the superior dots denote time derivatives; $\mu(S)$ = initial specific mass of tower (mass of a story divided by its height) at point of initial coordinate S; $\dot{s}(S)$ = velocity of material point with initial coordinate S. It will suffice to consider the velocity, as well as the momentum density, to be distributed throughout the compacted layer linearly. With these approximations, the crush-down differential equation of motion becomes:

$$\frac{\mathrm{d}}{\mathrm{d}t}\left\{m_0[1-\lambda(z)]\frac{\mathrm{d}z}{\mathrm{d}t}+\frac{\mu_c l}{2}[2-\lambda(z)]\frac{\mathrm{d}z}{\mathrm{d}t}\right\}-m(z)g=-F_c(z,\dot{z}) \quad \text{(crush-down)} \tag{2}$$

while the crush-up differential equation of motion has the same form as Eq. 17 of Bažant and Verdure (2007):

$$m(y)\left\{\frac{\mathrm{d}}{\mathrm{d}t}\left[[1-\lambda(y)]\frac{dy}{dt}\right]+g\right\}=F_c(y,\dot{y}) \qquad \text{(crush-up)} \tag{3}$$

Here Eq. (2) represents a refinement of Eq. 12 of Bažant and Verdure (2007), while Eq. (3) is identical to their Eq. 17 because the compacted layer is stationary during crush-up. Furthermore, l = height of compacted layer B, μ_c = specific mass of compacted layer B per unit height, which is considered to be constant and equal to the maximum possible density of compacted debris; $m(z)$ = cumulative mass of the tower above level z of the crushing front ($m(z) = m_0 + \mu_c l$); and F_c = resisting force = energy dissipation per unit height;

$$F_c(z,\dot{z}) = F_b + F_s + F_a + F_e, \quad F_b = W_d/(1-\lambda)h \tag{4}$$

where $W_d(z)$ = total energy dissipation up to level z, which was assumed by Bažant and Verdure (2007) to consist only of energy F_b (per unit height) consumed by buckling of steel columns.

In calculations, the large fluctuations of F_b as a function of z or y (evident in Figs. 3 and 4 of Bažant and Verdure, 2007) are neglected, i.e., F_b is smoothly homogenized. As a refinement of previous analysis, we introduce here a generalization in which we add energy F_s (per unit height) consumed by comminution of concrete floor slabs, energy F_a required to expel air from the tower, and energy F_e required to accelerate the mass of dust and larger fragments ejected from the tower during the impact of upper part; Furthermore, in contrast to previous studies, the compaction ratio will not be assumed as a constant but will be more accurately calculated as $\lambda(z) = (1-\kappa_{out})\mu(z)/\mu_c$, and κ_{out} = mass shedding fraction = fraction of mass that escapes outside tower perimeter before the end of crush-down (not afterwards).

Note that Eq. (2) may be rewritten as

$$[m_0(1-\lambda)+\mu_c l(1-0.5\lambda)]\ddot{z}-mg=-F_m-F_c, \quad F_m=[m_0(1-\lambda)+\mu_c l(1-0.5\lambda)]^{\cdot}\,\dot{z}=\bar{\mu}\dot{z}^2 \tag{5}$$

where F_m = force required to accelerate to velocity $\dot{z}$ the stationary mass accreting at the crushing front, and $\bar{\mu} = \mathrm{d}[m_0(1-\lambda)+\mu_c l(1-0.5\lambda)]/\mathrm{d}z$ = part of the impacted mass per unit height that remains within the tower perimeter. This force causes a greater difference from free fall than do forces F_b, F_s, F_a and F_e combined.

Upon setting $v = \dot{z}$, Eq. (2) or (5) was converted to a system of two nonlinear first-order differential equations for unknowns $v(t)$ and $z(t)$, which were then integrated numerically with high accuracy using the Runge-Kutta algorithm (note that, for the idealized special case of $\lambda = F_c = \kappa_{out} = 0$ and constant $\mu = \mathrm{d}m/\mathrm{d}z$, Eq. (2) reduces to the differential equation $(z\dot{z})^{\cdot} = gz$, which was formulated and solved by finite differences by Kausel, 2001). As the initial conditions, it is considered that the crushing front initiates at the 96$^{\text{th}}$ story in the North Tower, and at the 81$^{\text{st}}$ story in the South Tower (NIST 2005).

Based on video and seismic records, $\kappa_{out} \approx 0.2$, and based on the known typical density of rubble, $\mu_c = 4.10 \times 10^6$ kg/m. These are the values used to calculate the diagrams presented here. However, calculations have also been made for the full range of uncertainty of κ_{out}, as discussed later, and for μ_c ranging from 3.69×10^6 kg/m to 4.51×10^6 kg/m. Within these ranges, the changes in the results were not major.

Variation of Mass and Buckling Resistance along the Height

Near the top, the specific mass (mass per unit height) $\mu = 1.02 \times 10^6$ kg/m. In view of proportionality to the cross section area of columns, $\mu = 1.05 \times 10^6$ kg/m at the impact level (81^{st} floor) of South Tower. Although precise data on $\mu(z)$ are unavailable, it appears sufficient to use the approximation $\mu(z) = k_0 e^{k_2 z} + k_1$ (where k_0, k_1, k_2 = constants), with a smooth transition at the 81^{st} floor to a linear variation all the way down. The condition that $\int_0^H \mu(z)\mathrm{d}z$ be equal to the total mass of tower (known to be roughly 500,000 tons) gives $\mu = 1.46 \times 10^6$ kg/m at the base. There are various local complexities whose possible effects were estimated in calculations (e.g., the fact that 16 of 47 core columns at the bottom were much more massive than the rest). However, they appeared to have no appreciable effect on the overall response, particularly on the diagram of $z(t)$ and the collapse duration.

The total energy dissipation per unit height, which represents the resisting force F_c, consists not only of energy F_b dissipated by the inelastic hinges formed during column buckling, but also of energy F_s required for comminuting concrete floor slabs, energy F_a required for expelling air from the tower, and energy F_e required for ejecting particles and fragments. Based on Fig. 5 and Eq. 8 of Bažant and Zhou (2002), on Fig. 3 of Bažant and Verdure (2007), and on Bažant and Cedolin (2003, Sec 8.6), we have, for three-hinge column buckling:

$$F_b = \int_0^{u_f} \frac{F(u)\mathrm{d}u}{h}, \quad F(u) = \sum_{i=1}^{N} \frac{2[M_{ai}(\theta_i) + M_{bi}(\theta_i')]}{L_i \sin\theta_i}, \quad \theta_i = \arccos\left(1 - \frac{u}{L_i}\right) \tag{6}$$

where F = axial force resultant of all the columns in the story; u = vertical relative displacement between column ends, u_f = final u-value; $\theta_i' = 2\theta_i$; θ_i, θ_i' = hinge rotations at the ends and middle of column i, which are functions of u; M_{ai}, M_{bi} = bending moments in inelastic hinges at the ends and middle of column i, as functions of θ_i or θ_i'; and L_i = initial clear length of columns i. For plate-type four-hinge buckling (Fig. 2c in Bažant and Zhou 2002), similar simple expressions apply.

Although some core columns were rectangular, their plastic bending moments M_p were nearly proportional to the column cross section areas because, in the weak buckling direction, most core columns had the same width as the perimeter columns. Thus the curve $F(u)$ corresponding to perfect plasticity ($M_{ai} = M_{bi} = M_{p_i}$) is not difficult to estimate from the weight of all the columns in a story.

However, three effects doubtless intervened to reduce $F(u)$: 1) multi-story buckling of some columns; 2) softening due to local plastic flange buckling, and 3) fracture of steel in inelastic hinges (the last two likely occurred only at large buckling deflections for which $F(u)$ is small). The available data are insufficient to make an accurate estimate of these effects, and even the data on the flange thicknesses in the perimeter and core columns of all the stories are missing. So we simply apply to F_b an empirical correction factor β (≤ 1) which is reasonably expected to lie within the range (0.5, 0.8) for normal structural steel (yield limit 250 MPa), but in the range (0.1, 0.3) for the high-strength steel (yield limit 690 MPa) which was used for perimeter columns in the lower stories.

The high-strength steel has a much lower ductility, which must have caused fractures (with a drop of axial force to zero) very early during buckling, and must have been the cause of formation of large multistory fragments seen to fall from the lower part of tower. Consequently, the energy dissipated (which is equal to the area under the load-displacement curve of column) was probably about the same for high- and normal-strength columns.

The effect of uncertainty in F_b, i.e. $\beta = [0.5, 0.8]$, on the collapse time is shown in Fig. 8. The remaining diagrams are calculated with $\beta \approx 2/3$ for the stories with normal-strength column, while for high-strength columns, β is taken as 0.24, which gives about the same F_b as for normal-strength columns. But, for the stories with high-strength perimeter columns, the strength of core columns is 290 MPa (i.e., only slightly higher than for structural steel of normal strength). So we use $\beta \approx 0.2$ for these stories and expect the uncertainty range (0.1, 0.3). The full range of β will later be considered in estimating the uncertainty of response.

To estimate F_b, we consider that each perimeter column had a box cross section, almost square, with the width of 356 mm and web thickness varying from 7.5 mm near the top of tower to 125 mm near the bottom, while at the aircraft impact level the web was 10 mm thick (Wierzbicki and Teng 2003; Hart et al. 1985). The core columns had a rectangular box cross section from the tower base up to almost the top, where they had an I-section. The size of core

columns was not uniform even for a single story. Near the base, some reached 1371 mm × 559 mm, with wall thickness 127 mm (Engrg. News Record 1970). The cross section dimensions can be estimated, albeit only crudely, from recently released architectural blueprints.

Based on the area under the buckling curve in Fig. 3 of Bažant and Verdure (2007), the energy dissipation due to column buckling at the impact zone of the North Tower (96^{th} story) is $F_b(1-\lambda)h = 0.51$ GJ (or approximately 0.5 GJ, as estimated by Bažant and Zhou 2002). For other stories, this quantity is scaled according to the approximate cross section area of columns. For the sake of computational effectiveness, and because Eq. (2) is the continuum approximation of a difference equation, the variation of W_d/h is considered to be smooth, following a similar equation as that for $\mu(z)$.

Velocity of Air Ejected from the Tower

An upper bound on area through which the air initially contained within every story gets expelled (Fig. 3a) is $A_w = 4\psi a h_c$, where $4ah_c$ = area of one perimeter wall, $a = 64$ m = width of the side of square cross section of tower, $h_c = 3.69$ m = clear height of one story = distance from the bottom of a story slab to the top of the underlying slab, and ψ = vent ratio = ratio of unobstructed (open) area of the perimeter walls to their total area ($\psi \leq 1$). The initial mass of air within one story is $m_a = \rho_a a^2 h_c$, where $\rho_a = 1.225$ kg/m^3 = mass density of air at atmospheric pressure and room temperature. Just outside the tower perimeter, the air jetting out (Fig. 3a) must regain the atmospheric pressure as soon as it exits (White 1999, p.149), and its temperature must be roughly equal to the initial temperature (this is a well-known general feature of exhausts, e.g., from jet engines (White 1999, p.149) or pipes (Munson et al. 2006)). So, the mass density of exiting air $\rho \approx \rho_a$.

The time during which the top slab collapses onto the lower slab $\approx \Delta t = h_c/\dot{z}$ = time during which the air is expelled out (which is only about 0.07 s for stories near the ground). Conservation of the mass of air during the collapse of one story requires that $\rho A_w(v_a \Delta t) = \rho V_a$. Solving this equation gives the average velocity of escaping air just outside the tower perimeter:

$$v_a \;=\; \frac{V_a}{\psi A_w \Delta t} \;=\; \frac{a\dot{z}}{4\psi h_c} \tag{7}$$

Since the velocity of the crushing front near the end of North Tower crush-down is, according to the solution of Eq. (2), $\dot{z} = 47.34$ m/s (106 mph), the velocity of escaping air near the end of crush-down is

$$v_a = \frac{64\text{m} \;\times\; 47.34\text{m/s}}{4\psi \;\times\; 3.69\text{m}} = \begin{cases} 205\text{m/s (459 mph or 0.60 Mach)} & \text{for } \psi = 1 \\ 340\text{m/s (761 mph or 1.00 Mach)} & \text{for } \psi = 0.604 \end{cases} \tag{8}$$

The vent ratio ψ (which is < 1) is hard to estimate. It surely varies from story to story, and also during the crushing of one story. Its effective, or average, value could be much less than 1 (because some of the perimeter area is doubtless still obstructed early in the crushing of one story, and because much of the air escapes only after the story height has been reduced greatly). In spite of these uncertainties, it is clear that the exit air speed is of the order of 500 mph and that its fluctuations must reach the speed of sound. This must, of course, create sonic booms, which are easily mistaken for explosions (supersonic speeds are virtually impossible since the venting would require an orifice shaped similarly to a convergent-divergent nozzle).

There are other phenomena that can cause v_a to differ from the estimate in Eq. (8). The air pressure surely exhausts the load capacity of the floor slab for a few microseconds before it is impacted by the layer of compacted debris. So, the floor slab must crack before the story height is reduced to λh, and the air must begin to leak through the cracked floor slab into the underlying story, thus increasing the air mass in that story. Obviously some air must also leak into the ceiling which behaves as a porous layer of compacted gravel (it is impossible for the ceiling and the floor to remain flat and leak no air since otherwise the air pressure would tend to infinity as the ceiling impacts the floor).

All these complex inter-story interactions must cause rapid and large random fluctuations of internal air pressure and exiting air velocity. On the average, however, what matters is the simple fact that the air must, in one way or another, get expelled from each story of the tower within a very short time interval, which is only 0.07 s near the end of crush-down of North

Tower. This fact inevitably leads to the average exit velocity estimate in Eq. (7). The high velocity of air jetting out also explains why a large amount of pulverized concrete, drywalls and glass was ejected to a distance of several hundred meters from the tower (Fig. 3a).

Resisting Forces Due to Ejecting Air and Solids

The air mass within the confines of one story, which is $\rho_a a^2 h_c$, gets accelerated from 0 to velocity v_a as it exits the tower perimeter. The kinetic energy acquired by the escaping air of one story just outside the tower perimeter is $\mathcal{K}_a = \frac{1}{2}\rho {v_a}^2 (a^2 h_c)$ where $a^2 h_c$ = initial volume of air within the story.

The energy dissipated by viscosity of flowing air and by boundary friction is estimated to be negligible. Therefore, virtually all of the kinetic energy of escaping air must be supplied by gravity, and since the spatial derivative of energy is a force (called the material force or configurational force), the vertical resisting force caused by air ejection is

$$F_a(z, \dot{z}) \;=\; \frac{\mathcal{K}}{h} \;=\; \frac{\rho_a a^4}{32\psi^2 h_c h}\, \dot{z}^2 \tag{9}$$

Solution of Eq. (2) shows that, at the end of North Tower crush-down, $F_a \approx 103$ MN, which represents about 8.01% of the total resisting force F_c at the end of crush-down. When the first story under the aircraft impact zone gets smashed, F_a contributes only 2.75% of F_c. During the crush-down, the ratio F_a/F_c starts increasing and reaches the maximum of 12.79% when the 83^{rd} story gets impacted, and then decreases due to the increase of F_b at lower stories. $F_a <$ 5% of F_c up to the 3^{rd} story crushed, and $< 10\%$ up to the 7^{th} story crushed (by contrast, in building demolitions, which are conducted in the crush-up mode, the crush-up motion begins with zero velocity, and $F_a < 5\%$ of F_c for buildings up to about 20 stories tall, in which case the air resistance can be neglected). The maximum of F_a/F_c is 30.27%, which occurs during the crush-up phase in which F_b is small and the velocity high.

The average over-pressure of air within the tower is $\Delta p_a = F_a/a^2$ above the atmospheric pressure, which gives, for the North Tower, 7.55 kPa (0.075 atm), 14.31 kPa (0.141 atm) and 25.15 kPa (0.248 atm), respectively, during the crushing of the 80^{th} story, 50^{th} story, and at the end of crush-down, respectively. The last pressure value is enough to break up the floor slab. The pressure peaks near the end of squeezing of a story are doubtless much higher, as already mentioned, and thus must contribute to the break up of many floor slabs (theoretically, the pressure in a thin layer of viscous gas between two colliding parallel flat slabs approaches infinity at the end).

The mass that is shed from the tower, characterized by κ_{out}, exits at various velocities ranging from nearly 0 to almost either the air ejection velocity, for fine dust, or to roughly $\dot{z}$, for large steel pieces. Instead of complicating our model by some distribution of these velocities, we will simply assume that a certain fraction, $\kappa_e \kappa_{out}$, gets ejected in any direction (horizontal, inclined downward or upward, or almost vertical) at velocity $\dot{z}$, while the remaining mass $(1 - \kappa_e)\kappa_{out}$ is shed at nearly vanishing velocity. For a certain empirical value of κ_e, this must be energetically equivalent to considering the actual distribution of velocities of ejected solids. As the crushing front advances $\mathrm{d}z$, the mass of solids (dust plus large fragments) that is ejected at velocity $\dot{z}$ is $\kappa_e \kappa_{out} \mu(z) \mathrm{d}z$ and has kinetic energy $\kappa_e \kappa_{out} \mu(z)\ \mathrm{d}z(\dot{z}^2/2)$. This must be equal to $F_e \mathrm{d}z$, i.e., to the work of the resisting force F_e over distance $\mathrm{d}z$. It follows that

$$F_e \;=\; \tfrac{1}{2}\ \kappa_e \kappa_{out} \mu(z)\ \dot{z}^2 \tag{10}$$

The computation results shown in figures have been run for $\kappa_e = 0.2$; however, a broad range of κ_e has been considered in computations, as discussed later. For the crush-up, κ_e must be ignored because the compacted layer is stationary.

Energy Dissipated by Comminution (or Fragmentation and Pulverization)

The energy per unit height, F_s, that is dissipated by comminution of concrete floor slabs, can be calculated from the comminution theory, which is a subject well understood by now

(Schuhmann 1940; Charles 1957; Ouchterlony 2005; Cunningham 1987). The energy required for comminution is obviously proportional to the mass per unit height that is being comminuted, and is also known to depend of the relative velocity of impact, $\dot{z}$. Noting that the physical dimensions of F_s, mass per unit height and $\dot{z}$ are kg/s^2, kg/m and m/s, one readily concludes from dimensional analysis that $F_s \propto$ (mass per m)$\times \dot{z}^2$ is the only possible formula. Here the 'mass per m' is m_c/h because the mass that is being comminuted during crush-down of each story is not $m(z)$ but mass m_c of concrete floor of the story. So, F_s must have the form:

$$F_s \;=\; \gamma\, \frac{m_c}{2h}\, \dot{z}^2 \;=\; \gamma\, \frac{\mathcal{K}_c}{h} \tag{11}$$

where h is the height of one story and $\mathcal{K}_c = \frac{1}{2} m_c v^2 =$ kinetic energy of one floor slab if moving at velocity $v = \dot{z}$.

Coefficient γ (which is generally < 1 but not $\ll 1$) has been inserted in Eq. (11) as an empirical coefficient of comminution effectiveness, specifying the fraction of $\mathcal{K}_c$ that is dissipated by the work of comminution. The precise value of this coefficient would be extremely difficult to determine theoretically because all the other energy dissipation sources would have to be accurately calculated and subtracted from the total loss of gravitational potential converted into the kinetic energy of impact (these other sources include the energy of plastic-fracturing deformations of floor trusses with their connections and of horizontal steel beams connecting the perimeter columns, the energy dissipated by inelastic deformation and friction of colliding fragments, the energy of crushing the equipment, drywalls, perimeter walls, furniture, piping, etc.). Besides, the energy balance analysis is complicated by the fact that a part of the dissipated energy is included in force F_m, which must have, and does have, the same form as Eq. (5). The reason is that the equation of motion, Eq. (2), has been set up under the assumption that the accreted mass after impact gets moving together with the top part, which implies perfectly inelastic collision (or a zero coefficient of restitution).

For these reasons, and because no crushing experiments were made on the lightweight concrete used, coefficient γ needs to be calibrated on the basis of comminution theory, exploiting the known size range of particles observed after the collapse. Such calibration gives $\gamma = 0.7$ as the optimum estimate. For simplicity, we will further assume that $\gamma =$ constant, although it doubtless varies with z. It must nevertheless be emphasized that calculations prove the velocity of crush-down not to be very sensitive to the value of γ. For all $\gamma \in [0.5, 1]$, the calculated $z(t)$ matches the video and seismic observations considered later quite well (although $\gamma < 0.6$ would not give a close match of the observed particle distribution).

Consider that the mass, m_c, of concrete slab for each floor gets fractured into cubes of equal size D. The number of particles is $N = m_c/\rho D^3$ where $\rho =$ mass density of lightweight concrete (taken as 1500 kg/m^3). Since each cube has surface area $6D^2$ and each surface is common to two particles, the total energy required to create the particle surfaces is $\bar{W}_f = N(6D^2)G_F/2$.

The distribution of particle sizes is, for the present purpose, adequately characterized by Schuhmann's law of comminution (Schuhmann 1940; Charles 1957; Ouchterlony 2005; Cunningham 1987):

$$m(D) \;=\; m_c (D/D_{max})^k \tag{12}$$

where $m(D) =$ mass of all particles $< D$; $D_{max} =$ maximum particle size; and $k =$ empirical constant (for which the typical value $k \approx 1/2$ is assumed). The number of all particles within the size interval $(D, D + \mathrm{d}D)$ is $\mathrm{d}m/\rho D^3$, and so the energy required to create all the particles in this size interval is $(\mathrm{d}m/\rho D^3)(3D^2)G_F$; here $G_F =$ fracture energy of lightweight concrete, which is considered to be 20 J/m^2 (and is smaller than the value of 100 J/m^2 which is typical of normal concrete; Bažant and Planas 1998; Bažant and Becq-Giraudon 2002). In view of Eq. (12), the cumulative energy needed to create all the particles $< D$ is

$$W_f(D) \;=\; \int_{D_{min}}^{D} \frac{3G_F}{\rho D}\, \mathrm{d}m(D) \;=\; \frac{3kG_F m_c (D_{min}^{k-1} - D^{k-1})}{(1-k)\rho D_{max}^{k}} \tag{13}$$

where $D_{min} =$ minimum particle size.

The particle sizes observed on the ground range essentially from $D_{min} = 0.01$ mm to $D_{max} =$ 0.1 mm (see http://911research.wtc7.net/wtc/analysis/collapses/concrete.html). Substituting

$D = D_{max}$ = maximum particle size, and $W_f(D_{max}) = \gamma \mathcal{K}_c$, we get

$$\gamma = \frac{3G_F k}{\rho(1-k)\mathcal{E}D_{max}} \left[\left(\frac{D_{max}}{D_{min}} \right)^{1-k} - 1 \right], \qquad \mathcal{E} = \frac{\mathcal{K}_c}{m_c} \tag{14}$$

where $\mathcal{E}$ = specific impact energy (per kg of concrete). Substitution of the aforementioned particle sizes yields, for the end of crush-down, $\gamma \approx 0.7$, which is the aforementioned value used in the presently reported calculations.

Extensive experimental evidence indicates that the ratio D_{max}/D_{min} decreases as $\mathcal{E}$ increases (Ouchterlony 2005; Genc et al. 2004), being about 100 for small $\mathcal{E}$ characterizing the first impacted floor (Genc et al. 2004), and about 10 for high $\mathcal{E}$ characterizing the end of crush-down. The reason is that it is much harder to crush the small particles than the large ones. One may re-write Eq. (14) as

$$D_{max} = \frac{3G_F k}{\rho(1-k)\gamma\mathcal{E}} \left[\left(\frac{D_{max}}{D_{min}} \right)^{1-k} - 1 \right] \tag{15}$$

Substituting ratio 100 into Eq. (15), and evaluating $\mathcal{E}$ from the previously determined values $\mathcal{K}_c$ values, one gets the maximum and minimum particle sizes for the concrete slab of the first impacted floor,

$$\text{North Tower:} \quad D_{max} \approx 14.24 \text{ mm}, \quad D_{min} \approx 0.142 \text{ mm} \tag{16}$$

$$\text{South Tower:} \quad D_{max} \approx 12.76 \text{ mm}, \quad D_{min} \approx 0.128 \text{ mm} \tag{17}$$

Another important result of comminution theory, supported by extensive experiments (Davis and Ryan 1990), is that D_{max} depends only on the specific impact energy $\mathcal{E}$, and in particular that

$$D_{max} \;\approx\; A\, \mathcal{E}^{-p} \tag{18}$$

Here A, p = positive constants, which may be calibrated on the basis of the maximum particle sizes of the first impacted story and of the last story at the end of crush down. Substitution of Eq. (18) into (12) then yields the particle size distribution for any impacted floor slab;

$$\text{for North Tower:} \qquad m(D) = 0.021\ \mathcal{E}^{0.708} m_c\ \sqrt{D} \tag{19}$$

$$\text{for South Tower:} \qquad m(D) = 0.020\ \mathcal{E}^{0.712} m_c\ \sqrt{D} \tag{20}$$

Fig. 4a presents the calculated particle size distributions for the impacts on three different stories of each tower. Fig. 4b shows that the calculated minimum and maximum particle sizes produced by comminution of floor slabs decrease rapidly as the crushing front propagates down, and so does the size range. The ratio of the calculated mass of dust (defined here as the particles < 0.1 mm) to the slab mass increases with time until the end of crush-down (Fig. 4c). About 67% of the mass of all slabs gets pulverized into dust during the crush-down, which explains the dust clouds seen jetting out. Fig. 4d gives the ratio of the cumulative plot of the energy dissipated by comminution to the loss of gravitational potential, as a function of time or story number. The jump at impact of compacted layer on the ground (foundation) is due to further comminution of particles previously comminuted to larger sizes.

Fig.5a presents a plot of the calculated ratio of four components of the resisting force to the total resisting force F_c as a function of both time and story number. F_s, F_e and F_a as fractions of F_c are initially negligible and then increase, due to increasing velocity of the falling mass. Afterwards, despite increasing velocity, the increase of F_b offsets the increase of F_a, F_e and F_s. Consequently, fractions F_s, F_e and F_a begin to drop and, near the end of crush-down, $F_s + F_a + F_e \approx 0.30\ F_b$. At the same time, the falling mass becomes so huge that the effect of changes in F_s, F_a and F_e on the collapse duration becomes small. During the crush-up phase, the fraction of $F_s + F_a$ is significant at first, due to high velocity and low F_b of upper stories but afterwards it decreases as the falling mass decelerates ($F_s + F_a \approx 2.17\ F_b$ on average, while $F_e = 0$ for crush-up). Fig.5b shows the variation of F_c and F_m; due to increasing velocity, F_m becomes dominant despite increasing F_s, F_e and F_a.

Fig. 5c shows the calculated ratio of the comminution energy to the kinetic energy of the falling mass. During the crush-down, the ratio decreases, which is explained by the accretion

of falling mass. During the crush-up, this ratio increases since the falling mass is decreasing, and ends up with 70% as the last slab (i.e., the roof slab) impacts the pile.

Fig. 5d shows the calculated ratio of the total resisting force to the weight of the upper falling part. For the North Tower, this ratio remains almost constant up to the 83$^{\rm rd}$ story, as the mass accretion and the increase of F_c balance each other due to increasing velocity, and then increases because the resistance to column buckling overcomes the resistance due to mass accretion. This ratio is nevertheless much less than 1 during crush-down, while during crush-up it increases, causing the moving part to decelerate (a continuum model will give an infinite ratio at the end because the mass tends to 0). For the South Tower, the trend is similar except that this ratio at first also increases. The reason is that, compared to the North Tower, the calculated velocity of the crushing front in the South Tower increases faster, due to its larger falling mass, making the resisting force to grow faster than the mass accretion rate of the upper falling part at the beginning of crush-down.

Energy Required to Produce All of Pulverized Concrete

Let us now check whether the gravitational energy delivered by impact sufficed to produce the large amount of concrete dust on the ground. The dust particles generally ranged from D_{min} = 0.01 mm to D_{max} = 0.1 mm. Substituting $D = D_{max}$ into Eq. (13), and considering, as an upper bound, that all of the concrete of both towers (about $M_d = 14.6 \times 10^7$ kg) was pulverized, lying on the ground, we can calculate an upper bound on the total impact energy $\mathcal{K}_t$ required to produce all these particles, for both towers:

$$\mathcal{K}_t = \frac{3 M_d G_F}{\rho D_{max}^{0.5}} (D_{min}^{-0.5} - D_{max}^{-0.5}) \tag{21}$$

$$= \frac{3 \times (14.6 \times 10^7) \text{ kg} \times 20 \text{ J/m}^2}{1500 \text{ kg/m}^3 \times (100 \ \mu\text{m})^{0.5}} [(10 \ \mu\text{m})^{-0.5} - (100 \ \mu\text{m})^{-0.5}] = 12.63 \times 10^{10} \text{ J} \tag{22}$$

Eq. (21) indicates the dissipation of about 865 J per kg of pulverized concrete, which is a realistic value.

The total gravitational potential energy Π_g released by one tower is calculated as the tower weight multiplied by the distance between the mass centroid of the tower and the mass centroid of the rubble heap on the ground, and is approximately $\Pi_g = 8.25 \times 10^{11}$ J. Eq. (21) represents only about 7.65 % of $2\Pi_g$ (both towers). So there is far more impact energy than necessary. Hence, the kinetic energy of gravity-driven collapse can perfectly explain the pulverization seen on the ground. The remaining energy is dissipated by frictional and plastic deformations, and ejection of air and other debris.

Eq. (21) includes the comminution energy during the crush-down and crush-up. The energy dissipated exclusively during the impact on the foundation can be calculated by subtracting from Eq. (21) the following three energy quantities: 1) The comminution energy of particles $<$ 0.1 mm produced by impacts on the floor slabs prior to the end of crush-down; 2) the comminution energy of particles $\geq$ 0.1 mm produced during crush-down which are comminuted to sizes $<$ 0.1 mm during the impact on the foundation; and 3) the comminution energy of particles $<$ 0.1 mm produced during the crush-up (which is small because the impact energies during crush-up are much smaller and lead to large fragments).

The kinetic energy of the impact, K_t, can alternatively be calculated from the final velocity v_f of the compacted layer of rubble as it hits the foundation at the bottom of the 'bathtub'. According to the crush-down differential equation, it was $v_f \approx 47.34$ m/s for the North Tower, and $v_f \approx 48.33$ m/s for the South Tower), from which

$$K_t = \tfrac{1}{2}[M_0 + (1 - \kappa_{out})(M_T - M_0)] {v_f}^2 \tag{23}$$

$$\text{North Tower:} \quad K_t = \tfrac{1}{2} \times 4.32 \times 10^8 \times 47.34^2 = 4.84 \times 10^{11} \text{ J} \tag{24}$$

$$\text{South Tower:} \quad K_t = \tfrac{1}{2} \times 4.44 \times 10^8 \times 48.33^2 = 5.19 \times 10^{11} \text{ J} \tag{25}$$

We see again that the available energy is far higher than required for all of the comminution.

It is nevertheless interesting to check the amount of explosives that would be required to produce all of the pulverized concrete dust found on the ground. Explosives are notoriously inefficient as a comminution tool. At most 10% of their explosive energy gets converted into the fracture energy of comminution, and only if the explosive charges are installed in small holes drilled into the solid to be comminuted. Noting that 1 kg of TNT releases chemically about 4 MJ of energy, the total mass of TNT required to pulverize 14.6×10^7 kg concrete material into dust of the sizes found on the ground would be 316 tons. So, in order to achieve solely by explosives the documented degree of concrete pulverization, about 1.36 tons of TNT per story would have to be installed into small holes drilled into the concrete slab of each story, and then wired to explode in a precise time sequence to simulate free fall.

Given the uncertainty of input parameters, computer calculations have been run for the full range of their realistic values. In comparison with all these calculations, the claim that the observed fineness, extent and spread of pulverized dust could be explained only by planted explosives has been found to be absurd. Only gravity driven impact could have produced the concrete dust as found on the ground.

Analysis of Video-Recorded Motion and Correction for Tilt

Some critics believe that the bottom of the advancing dust cloud seen in the video represented the crushing front. However, this belief cannot be correct because the compressed air exiting the tower is free to expand in all directions, including the downward direction. This must have caused the dust front to move ahead of the crushing front (the only way to prevent the air from jetting out in all directions would be to shape the exit from each floor as a diverging nozzle of a rocket, which was obviously not the case).

Video records in which the motion of the tower top can be tracked are available for the first few seconds, until the tower top gets shrouded by a cloud of dust and smoke (Fig. 7). The time history of the vertical displacement (or drop) Δ_m of the tower top was simply identified by measurements with a ruler on a large computer screen, which had an error of up to ± 1.0 m (measuring pixel locations would have been more accurate, but for the present purpose it would make little difference). A correction was made for the varying inclination φ of the line of sight from the vertical, and for this purpose the distance of the camera from the tower ($\approx$ 1 mile) and altitude (roughly 150 m) had to be estimated. This correction was found to be insignificant (about 0.5%.) Because the towers were tilting, what can be seen in the video is a top corner, which is the northeast corner for the South Tower and the northwest corner for the North Tower. With the notations in Fig. 6a, the height of these corners above the ground may be expressed as

$$X(t) = H - Y(t) + \Delta_{1c}(t) - \Delta_{2c}(t) \tag{26}$$

$$Y(t) = \int_{z_0}^{z(t)} [1 - \lambda(S)] \mathrm{d}S \tag{27}$$

$$\Delta_{1c}(t) = \tfrac{1}{2} a \ (\sin\theta_{st} - \sin\theta_{si} - \sin\theta_{et} + \sin\theta_{ei}) \tag{28}$$

$$\Delta_{2c}(t) = \tfrac{1}{2} H_1 \ [(\cos\theta_{si} - \cos\theta_{st}) + (\cos\theta_{ei} - \cos\theta_{et})] \tag{29}$$

where $Y(t)$ = drop of the centroid of the upper falling mass; Δ_{1c}, Δ_{2c} = corrections for tilting; θ_{si}, θ_{st} = initial and current tilt angles towards the south; and θ_{ei}, θ_{et} = those towards the east (these angles are taken as positive when the displacement is downward on the south and east sides, respectively; Fig. 6a).

For the South Tower, $H_1 \approx 110$ m. It is found that, during the the first 2 seconds, the tilt towards the east increased from 2.8° to 6.9°. In between, the rate of rotation may be considered to be approximately uniform. According to NIST 2005, the tilt towards the south reached 4° within approximately 2 seconds. For the initial tilt angle towards the south, no information exists except that it could not have been large, and so it is taken as zero. For the duration of video record, the foregoing equations give the correction of height due to tilt, which attains 0.48 m at 2 seconds (the video record actually extends up to 4 s, at which time, according to NIST, the tilt angle to the East was 25° and to the South probably remained small). Thus the tilt after 2 s is too high for comparing the present one-dimensional model to the video, although this model appears adequate for the overall collapse.

For the North Tower, it was assumed in the calculations that the tilt in the south direction varied during the first 5 seconds from 2.8° to 8° (which is the angle reported by NIST 2005), and that it was zero in the east direction.

The motion of the centroid of the tower tops identified in this manner is shown Fig. 7. The vertical error bars indicate the range of uncertainty in the interpretation of the video.

Comparisons of Calculated Motion with Video Record

The corrections for tilt in Eqs. (26)–(29) are taken into account in the calculations. Since there are uncertainties in the values of specific mass of compacted layer μ_c and the mass shedding ratio κ_{out}, calculations are run for many values within their possible ranges. For μ_c, the uncertainty range is $4.10 \times 10^6 \pm 0.410 \times 10^6$ kg/m, based on regarding the compacted rubble as gravel, for which the realistic value of porosity is well known from soil mechanics. As for κ_{out}, the fits of the video and seismic records are optimal for 0.2, but the optimum is not sharp. For $\kappa_{out} \in [0.05, 0.5]$, the results are within the error bars if μ_c is set to 4.10×10^6 kg/m. If both μ_c and κ_{out} are considered to vary, then the results remain within the error bars if $\kappa_{out} \in [0.1, 0.3]$. The range plotted in Fig. 7 corresponds to $\mu_c \in [3.69 \times 10^6, 4.51 \times 10^6]$ (kg/m) and $\kappa_{out} \in [0.1, 0.3]$.

The range of the possible motion histories, calculated from Eq. (2) for the uncertainty ranges of video interpretation and of μ_c and κ_{out} values (discussed later) is shown as the shaded band in Fig. 7. Within the short duration of the video record, the resistance due to comminuting concrete and ejecting air and other debris is found to be so small that the difference is not visually perceptible in the graph.

Note in Fig. 7 that the motion identified from the videos is generally seen to pass well inside the predicted band of uncertainty of the motion calculated from Eq. (2). This fact supports the present analysis. The main point to note is that the curve identified from the video record grossly disagrees with the free fall curve, for each tower. The belief that the towers collapsed at the rate of free fall has been a main argument of the critics claiming controlled demolition. The video record alone suffices to prove this argument false.

For the South Tower, the difference between the free fall curve and the curve calculated from Eq. (2) is less pronounced than it is for the North Tower. The reason is that the initial upper falling mass of the South Tower is nearly twice that of the North Tower, causing the resisting force to be initially a smaller fraction of the falling weight.

The agreement of the video record with the calculated propagation of crushing front permits concluding that the structural system within the top parts of the WTC towers was able, on the average, to dissipate the energy of $F_b \approx 0.1$ GJ/m, per unit height of tower. This amounts to the energy dissipation capability of $\mathcal{D} \approx 4.23$ kJ per kg of structural steel.

In design, it is desirable to maximize $\mathcal{D}$. As proposed in Bažant and Verdure (2007), the values of $\mathcal{D}$ characterizing various kinds of structural systems could be determined by accurate monitoring of the motion history in building demolitions.

Comparison of Collapse Duration with Seismic Record

Calculations show that the duration of the entire crush-down phase exceeds the free fall duration by 65.5% for the North Tower, and by 47.3% for the South Tower (Fig. 8). This is a significant difference, which can be checked against seismic records registered at Lamont-Doherty Earth Observatory of Columbia University (http://www.ldeo.columbia.edu/LCSN/Eq/WTC_20010911.html), shown in Fig. 8. In a detailed seismic analysis at Columbia University, Kim et al. (2001) report that, because of short travel distance and shallow excitation, the recorded seismic waves were short-period Rayleigh surface waves (which generally travel within the upper few kilometers of Earth crust). No pressure and shear waves were registered.

The first tremor in Fig. 8, which is weak (and is marked as a), is assumed to represent $t = 0$, i.e., the moment of impact of the upper part of tower onto the lower part (a correction of 0.07 s is made for the delay due to the travel time of the sound wave along the steel columns to the ground). The sudden, though mild, displacement increase at instant b (Fig. 8) is attributed to free falling large structure segments that hit the ground outside the tower perimeter.

The free fall times for the fragments ejected at the 96^{th} and 81^{st} stories are 8.61 s and 7.91 s, respectively (the air drag is negligible for multi-story pieces of the steel frame). These times

are not the same as the free fall time shown in the Fig. 8, because the ejected fragments are hitting the ground. The free fall curve in Fig. 8, showing the motion history of the tower top, corresponds to the free fall of the top part of tower, and the moment comparable to the end of crush-down is the intersection of this curve with the horizontal line corresponding to the end of crush-down, at which the compacted layer of debris hits the foundation (i.e., the bottom of 'bathtub'). Note that immediately after this moment, the compacted layer of rubble begins to spread to the sides because, at rest, the slope of the rubble mass cannot exceed the internal friction angle of the rubble (Fig. 3b)(in the crush-up calculations of Bažant and Verdure, 2007, the lateral spreading of the compacted layer of rubble during the crush-up was neglected, for the sake of simplicity).

The onset of the strongest tremor, marked in the figure as instant c, may logically be interpreted as the instant at which the crush-down front (bottom of the layer of compacted debris) hits the foundation slab in the 'bathtub'. Thus it ensues from the seismic records that the crush-down phase lasted 12.59 ± 0.50 s for the North Tower, and 10.09 ± 0.50 s for the South Tower. The fact that the structure in the 'bathtub' under the ground level was essentially destroyed and mostly compacted into rubble was documented during debris removal (http://www.construction.com/NewsCenter/Headlines/ENR/20011008b.asp).

These durations match reasonably well the durations of the crush-down phase calculated from Eq. (2), which are 12.81 s and 10.47 s for the North and South towers, under the assumption that the reduction factor β applied to F_b is 2/3. If the full uncertainty range, $\beta \in [0.5, 0.8]$, is considered, the calculated mean durations are 12.82 s and 10.49 s, respectively. This uncertainty is shown by error bars in Fig. 8.

Now note that these durations are, on the average, 65.5% and 47.3% longer than those of a free fall of the upper part of each tower, which are 7.74 s for the North Tower and 7.11 s for the South Tower. So, the seismic record, too, appears to contradict the hypothesis of progressive demolition by timed explosives.

Note that the seismic record of the South Tower shows multiple large tremors at the end of crush-down. Why it does is debatable. The reason could be the significant tilting of the top part of tower, caused by a greater eccentricity of the aircraft impact. The tilt may have led to ejection of larger structural fragments. Or it may have caused one side of the South Tower to be getting crushed ahead of the other, and thus the crush-down might have ended on one side earlier than on the other. It is interesting that not only for the North Tower, but also for the South Tower, the calculated collapse duration nevertheless matches the seismic record reasonably well. The high tilt seen on the South Tower top (about 25° after 4 seconds of fall, NIST 2005) would call for a three-dimensional model of progressive collapse. Why does the one-dimensional model give nonetheless a reasonably good match? Probably because the crushing front of compacted debris tends to develop a flat front once it becomes thick enough (Fig. 6e). However, to answer this question fully, a three-dimensional analysis would be required.

Effect of Uncertainty of Mass Shedding Fraction κ_{out}

The mass shedding fraction κ_{out} is, of course, quite uncertain and doubtless depends on z, which is neglected. The realistic range of possible κ_{out} values extends at most from 0.05 to 0.5. Within that range, the effect of varying κ_{out} is not discernible in the video (remaining within the error bars shown), and small on the collapse time (which differs up to 0.45 s). For $\kappa_{out} \in [0.1, 0.3]$, the match of both the video and seismic records is excellent.

While κ_{out} affects the resisting force, mass accretion, and compaction ratio, κ_e affects only the first. An increase in κ_e will delay the collapse duration. Parametric studies show that, for $\kappa_e \in [0.1, 0.8]$, the collapse duration varies about 0.31 s, which still matches the video and seismic records reasonably well. An increase in κ_{out} can have opposite effects depending on the initial mass $m(z_0)$ and on the stage of crush-down:

(a) In the first stage of collapse, an increase in κ_{out} causes a decrease in compaction ratio λ, which reduces the acceleration of the crush front. The effect of κ_{out} on the resisting force and mass accretion is not dominant in this stage. This gives a slower collapse.

(b) For a subsequent short stage of crush-down, the effect of κ_{out} on the resisting force F_m prevails while the effect of κ_{out} on the mass accretion does not. This gives a faster collapse.

(c) In the late stage of crush-down, an increase in κ_{out} causes the accumulated mass $m(z)$ to become significantly smaller, while the column crushing force F_b remains unchanged. This causes the ratios $m(z)g/F_b$, and thus also $m(z)g/F_c$, to decrease greatly, which gives a slower

collapse.

Parametric studies show that stage (a) lasts for 2 to 3 s. The role of stages (b) and (c) in the total collapse duration depends on the initial falling mass m_0. For the North Tower, because of its lower initial falling mass, stage (c) dominates, and so an increase in κ_{out} always gives an increase in collapse duration. If κ_{out} is increased from 0.05 to 0.5, the crush-down collapse duration is longer, but not by more than 0.45 s, which still matches the seismic record well enough. For the South Tower, the effect of stage (b) mildly prevails over a considerably long period while effects of stages (a) and (c) are weak. The net result is to lengthen the crush-down duration, but only a little; if κ_{out} is varied from 0.05 to 0.5, the crush-down duration increases by only 0.14 s. For the fitting of video record of the first few seconds, the velocity is so low that the effect of κ_{out} is imperceptible, for both towers.

Some lay critics claim that κ_{out} should be about 95%, in the (mistaken) belief that this would give a faster collapse and thus vindicate their allegation of free fall. However, such κ_{out} value would actually extend the duration of collapse of North Tower by about 2.11 s (and 1.50 s for $\kappa_{out} = 90\%$) because the effect of stage (c) would become dominant. Agreement with the seismic record would thus be lost. This is one reason why values $\kappa_{out} > 0.5$ are unrealistic.

These lay critics claim that the mass shedding fraction κ_{out} was about the same as the percentage of rubble found after the collapse outside the footprint of the tower. The maximum estimate of this percentage is indeed 95%. However, aside from the comparisons with video and seismic records, there are four further reasons indicating that a major portion of the rubble seen on the ground after the collapse must have spread outside the tower footprint only after the crush-down, i.e., after the impact of the falling compacted layer onto the ground:

1) One is a physical analogy with the mechanics of rigid foams. Compressing an object in one direction expels mass laterally only if the compressed object consists of a volumetrically incompressible mass, as in compressing clay. But, if the object has much empty space, as in the case of the twin towers, one must expect a similar behavior as in penetration of a hard missile into a rigid foam, in which case almost no mass is spread laterally.

2) The large steel fragments move virtually in a free fall, much faster than the dust. If κ_{out} were almost 1, many of them would be expected to move ahead of the lower margin of dust cloud. Yet the photographs show the density of falling steel fragments visible in the air to be far too small to account for most of the mass of the steel frame.

3) If most of the mass were falling in the air outside the tower perimeter, one would have to expect a seismic signal with continuous mild tremors, in which the arrival of the crushing front to the ground would not be clearly differentiated. But it is.

4) One may also consider the dust density in the cloud. For the first two stories of collapse (i.e., first 1.3 second), the cloud volume seen in the photos can be approximated as the volume of four half-cylinders with horizontal axis and diameters equal to the height of two stories and lengths equal to the tower side. This gives about 6000 m^3. On the ground, the dust density was reported by EPA (Environmental Protection Agency) to be about 339 kg/m^3. But in the air, the average dust density could not have been more than 10% of the dust density on the ground; this gives, for the dust portion of κ_{out}, at most 0.05, during the first 1.3 s of collapse.

As for the crush-up phase, κ_{out} has no effect on the equation of motion but affects the initial condition, which is the final velocity of crush-down phase. It is found that increasing κ_{out} reduces the final velocity and extends the crush-up duration.

Previously Refuted Hypotheses of Critics

Some other hypotheses have already been refuted in the discussions at the U.S. National Congress of Theoretical and Applied Mechanics in Boulder, June 2006. This includes the hypothesis that the structural frame was somehow brought to the brink of strain-softening damage and then destroyed by a peculiar phenomenon called the "fracture wave", causing the collapse to occur at the rate of free fall (download Progre...pdf from http://www.civil.northwestern.edu/people/bazant/PDFs/Papers/). There are three serious problems with this hypothesis: 1) It treats strain-softening as a local, rather than nonlocal, phenomenon (Bažant and Verdure 2007); 2) it considers the structural frame to have somehow been brought to a uniform state on the brink of strain softening, which is impossible because such a state is unstable and localizes as soon as the strain softening threshold at any place (Bažant and Cedolin 2003, Sec 13.2); 3) the 'fracture wave' is supposed to cause comminution of concrete but the energy required for comminution cannot be delivered by this wave.

Another previously refuted hypothesis of the lay critics is that, without explosives, the towers would have had to topple like a tree, pivoting about the base (Bažant and Zhou 2002) (Fig. 6b or c). This hypothesis was allegedly supported by the observed tilt of the upper part of tower at the beginning of collapse (Fig. 6a). However, rotation about a point at the base of the upper part (Fig. 6c) would cause a horizontal reaction approximately 10.3× greater than the horizontal shear capacity of the story, and the shear capacity must have been exceeded already at the tilt of only 2.8° (Bažant and Zhou 2002). Thereafter, the top part must have been rotating essentially about its centroid, which must have been falling almost vertically. The rotation rate must have decreased during the collapse as further stationary mass accreted to the moving block. So, it is no surprise at all that the towers collapsed essentially on their footprint. Gravity alone must have caused just that (Bažant and Zhou 2002).

In the structural engineering community, one early speculation was that, because of a supposedly insufficient strength of the connections between the floor trusses and the columns, the floors 'pancaked' first, leaving an empty framed tube, which lost stability only later. This hypothesis, however, was invalidated at NIST by careful examination of the photographic record, which shows some perimeter columns to be deflected by up to 1.4 m inward. This cannot be explained by a difference in thermal expansion of the opposite flanges of column. NIST explains this deflection by a horizontal pull from catenary action of sagging floor trusses, the cause of which has already been discussed. This pull would have been impossible if the floor trusses disconnected from the perimeter columns.

Other critics claimed sightings of "pools of molten metal" within the rubble pile, purportedly produced by planted thermite-based incendiary devices. But all of the supposed evidence is entirely anecdotal, and is refuted by the facts in NIST (2005) report. It was asserted that the presence of thermite residues was evidenced by sulfur, copper and zinc detected in the WTC dust samples. But these elements were to be expected since they were contained in gypsum wallboard, electrical wiring, galvanized sheet steel, etc.

Conclusions

Several of the parameters of the present mathematical model have a large range of uncertainty. However, the solution exhibits small sensitivity to some of them, and the values of others can be fixed on the basis of observations or physical analysis. One and the same mathematical model, with one and the same set of parameters, is shown capable of matching all of the observations, including: (1) the video records of the first few seconds of motion of both towers, (2) the seismic records for both towers, (3) the mass and size distributions of the comminuted particles of concrete, (4) the energy requirement for the comminution that occurred, (5) the wide spread of the fine dust around the tower, (6) the loud booms heard during collapse, (7) the fast expansion of dust clouds during collapse, and (8) the dust content of cloud implied by its size. At the same time, the alternative allegations of some kind of controlled demolition are shown to be totally out of range of the present mathematical model, even if the full range of parameter uncertainties is considered.

These conclusions show the allegations of controlled demolition to be absurd and leave no doubt that the towers failed due to gravity-driven progressive collapse triggered by the effects of fire.

Appendix. Can Crush-Up Proceed Simultaneously with Crush-Down?

To appraise the accuracy of the simplifying assumption of one-way crushing, a two-way progressive collapse will not be analyzed mathematically. Consider that both crush-up and crush-down fronts appeared after the collapse of the critical story. Denote: $x(t), z(t)$ = coordinates of the mass points at these fronts before the collapse began (Lagrangian coordinates); $q(t)$ = current coordinate of the tower top; and v_1, v_2 = initial velocities of the downward and upward crushing fronts (positive if downward). These velocities may be calculated from the conditions of conservation of momentum and of energy, which read as follows:

$$\begin{aligned} &m_0(1-\lambda)v_0 + \tfrac{1}{2}m_1[(1-\lambda)v_0 + v_0] \\ &\quad = \tfrac{1}{2}(m_1+2m_c)(v_1+v_2) + (m_0 - m_c - m_2)v_3 + \tfrac{1}{2}m_2(v_1+v_2) \\ &\tfrac{1}{2}m_0[(1-\lambda)v_0]^2 + \tfrac{1}{2}m_1[\tfrac{1}{2}(2-\lambda)v_0]^2 \end{aligned} \tag{30}$$

$$= \tfrac{1}{2}(m_1+2m_c)[\tfrac{1}{2}(v_1+v_2)]^2 + \tfrac{1}{2}(m_0-m_c-m_2)v_3^2 + \tfrac{1}{2}m_2[\tfrac{1}{2}(v_1+v_2)]^2 + \Delta E_c \qquad (31)$$

Here $v_3 = \dot{q} = (1-\lambda)(v_1+v_{cu})$ where $v_{cu} = [(1-\lambda)v_1 - v_2]/\lambda$ = initial crush-up velocity (positive if upwards); m_c = mass of one floor slab; m_0, m_1 = masses of the upper part C and of the story that was the first to collapse (not including the floor slab masses), m_2 = mass of a single story; and ΔE_c = energy loss due to comminution of materials, predominantly concrete, into small fragments during impact, which has been calculated as $0.35m_c(v_1^2 + v_{cu}^2)$ using the theory of comminution (i.e. $\Delta E_c = 0.5\gamma m_c v^2$ where $\gamma = 0.7$). In Eqs. (30) and (31), it is assumed that the momentum density varies linearly throughout the compacted layer B, and that, when the crushing front starts to propagate upwards, the falling part C moves downwards as a rigid body except that its lowest story has momentum density varying linearly (i.e. homogenized) throughout the story.

During impact, $\lambda = 0.2$ for the North Tower and 0.205 for the South Tower, as calculated from the mass of the impacted story and the debris density. For the North or South Tower: $m_0 = 54.18 \cdot 10^6$ or $112.80 \cdot 10^6$ kg, $m_1 = 2.60 \cdot 10^6$ or $2.68 \cdot 10^6$ kg, $m_2 = 3.87 \cdot 10^6$ or $3.98 \cdot 10^6$ kg, and $m_c = 0.627 \cdot 10^6$ kg for both. For a fall through the height of the critical story, by solving Eq. 2, one obtains the crush-front velocity $v_0 = 8.5$ m/s for the North Tower and 8.97 m/s for the South Tower. The solution of Eqs. (30) and (31) yields the following velocities after impact: $v_1 = 6.43$ or 6.8 m/s, $v_2 = 4.70$ or 4.94 m/s, and $v_{cu} = 2.23$ or 2.25 m/s for the North or South Tower, respectively. These data are used as initial conditions for the differential equations of motion of the upper part C and of the compacted layer B. These equations represent generalizations of Eq. (2) and (3), and can be shown to have the form:

$$\frac{\mu_c}{2}\,\frac{\mathrm{d}}{\mathrm{d}t}\left(\{[2-\lambda(z)]\dot{z} + \lambda(x)\dot{x}\}l\right) = \mu_c l g + F_c' - F_c \qquad (32)$$

$$\frac{\mathrm{d}}{\mathrm{d}t}\left(m(x)\{[1-\lambda(z)]\dot{z} - [1-\lambda(x)]\dot{x}\} + \frac{m_2}{2}\,\dot{x}\right) = m(x)g - F_c' \qquad (33)$$

where $l = \int_x^z \lambda(S)\mathrm{d}S$ = current height of the compacted layer of rubble; $m(x) = \int_0^x \mu(S)\mathrm{d}S$ = all the mass above level x, and F_c and F_c' are the normal forces in the crush-down and crush-up fronts calculated according to Eq. 4. The actual resisting column force is used in the calculations. The cold steel strength is used for the story below the critical one, and a 15% reduction in steel strength due to heating is assumed for the story above the critical one.

Fig. 9 shows the calculated evolution of velocity and displacement in the two-way crush. As seen, the crush-up stops (i.e. $|\dot{x}|$ drops to zero) when the first overlying story is squashed by the distance of only about 1% of its original height for the North Tower, and only 0.7% for the South Tower (these values are, respectively, about 11 or 8 times greater than the elastic limit of column deformation). Why is the distance smaller for the South Tower even though the falling upper part is much more massive? That is because the initial crush-up velocity is similar for both towers while the columns are much stronger (in proportion to the weight carried). Since the initial crush-up phase terminates at very small axial deformation, it must be concluded that the simplifying hypothesis of one-way crushing is perfectly justified and causes only an imperceptible difference in results.

If random fluctuation of column strength is taken into account, the crush-up resisting force F_c' in the first overlying story may be lower or higher than indicated by the foregoing deterministic analysis. If it is lower, the crush-up will penetrate deeper. But even for the maximum imaginable standard deviation of the average column strength in a story, the crush-up will get arrested before it penetrates the full story height.

Acknowledgment. *Partial financial support for the energetic theory of progressive collapse was obtained from the U.S. Department of Transportation through grant 0740-357-A210 of the Infrastructure Technology Institute of Northwestern University. Richard M. Lueptow, professor at Northwestern University, and Pierre-Normand Houle of Montreal, are thanked for useful comments.*

References

[1] Bažant, Z.P. (2001). "Why did the World Trade Center collapse?" *SIAM News* (Society for Industrial and Applied Mathematics) Vol. 34, No. 8 (October), pp. 1 and 3 (submitted Sept. 13,

2001).

[2] Bažant, Z.P., and Becq-Giraudon, E. (2002). "Statistical prediction of fracture parameters of concrete and implications for choice of testing standard." *Cement and Concrete Research* 32 (4), 529–556.

[3] Bažant, Z.P., and Cedolin, L. (2003). *Stability of Structures: Elastic, Inelastic, Fracture and Damage Theories*, 2nd ed., Dover Publications (catalog No. 42568-1), New York.

[4] Bažant, Z.P., Le, J.-L., Greening, F.R., and Benson, D.B. (2007). "Collapse of world trade center towers: what did and did not cause it?" *Structural Engrg. Report* 07-05/C605c, Northwestern University, Evanston, Illinois.

[5] Bažant, Z.P. and Le, J.-L. (2008). "Closure to "Mechanics of Progressive Collapse: Learning from World Trade Center and Building Demolitions" by Zdeněk P. Bažant and Mathieu Verdure ", *Journal of Engineering Mechanics, ASCE* 134, 2008; in press.

[6] Bažant, Z.P., and Planas, J. (1998). *Fracture and Size Effect in Concrete and Other Quasibrittle Materials*. CRC Press, Boca Raton and London.

[7] Bažant, Z.P., and Verdure, M. (2007). "Mechanics of Progressive Collapse: Learning from World Trade Center and Building Demolitions." *J. of Engrg. Mechanics ASCE* 133, pp. 308–319.

[8] Bažant, Z.P., and Zhou, Y. (2002). "Why did the World Trade Center collapse?—Simple analysis." *J. of Engrg. Mechanics ASCE* 128 (No. 1), 2–6; with Addendum, March (No. 3), 369–370 (submitted Sept. 13, 2001, revised Oct. 5, 2001).

[9] Charles, R. J. (1957)."Energy-size reduction relationships in comminution" *Mining Engrg.* 9, 80–88.

[10] Cunningham, C.V.B. (1987). "Fragmentation estimation and the Kuz-Ram model—four years on." *Proc., 2nd Int. Symp. on Rock Fragmentation by Blasting* (held in Bethel, Connecticut), W.L. Fourney & R.D. Dick, Eds., SEM, pp. 475-487.

[11] Davis, D.R., and Ryan, E.V. (1990). "On collisional disruption: experimenal results and scaling law" *ICARUS.* 83, 156-182.

[12] Frost, H. J. and Ashby, M.F. (1982). *Deformation-Mechanism Maps The Plasticity and Creep of Metals and Ceramics*. Pergamon Press (Sec. 8).

[13] Genc, O., Ergün, L., and Benzer, H. (2004). "Single particle impact breakage chacterization of materials by drop testing" *Physicochemical problems of Mineral Processing.* 38, 214-255.

[14] Hart, F., Henn, W., and Sontag, H. *Multi-story buildings in steel* Cambridge, UK: Univeristy Press, 1985.

[15] Kausel, E. (2001). "Inferno at the World Trade Center", *Tech Talk (Sept. 23)*, M.I.T., Cambridge.

[16] Kim, W.-Y., Sykes, L.R., Armitage, J.H., Xie, J.K., Jacob, K.H., Richards, P.G., West, M., Waldhauser, F., Armbruster, J., Seeber, L., Du, W.X., and Lerner-Lam, A. (2001). "Seismic waves generated by aircrafts impacts and building collapses at World Trader Center, New York City."*EOS, Transaction American Geophysical Union*, Vol 82, 47, 565-573.

[17] Levy, M., and Salvadori, M. (1992). *Why buildings fall down?* W.W. Norton, New York.

[18] Munson, B.R., Young, D.F., and Okiishi, T.F. (2006). "Fundamentals of Fluid Mechanics," 5th ed., J. Wiley, Hoboken, NJ.

[19] NIST (2005). *Final Report on the Collapse of the World Trade Center Towers*. S. Shyam Sunder, Lead Investigator. NIST (National Institute of Standards and Technology), Gaithersburg, MD (248 pgs.)

[20] Ouchterlony, F. (2005). "The Swebrec function: linking fragmentation by blasting and crushing." *Mining Technology* 114 (March), pp. A29–A44.

[21] Schuhmann, R. Jr. (1940). "Principles of comminution, I. Size distribution and surface calculation". *The American Institute of Mining, Metallurgical, and Petroleum Engineers (AIME) Technical Publication* 1189.

[22] White, F.M. (1999). *Fluid Mechanics*, 4th ed., WCB/McGraw-Hill, Boston (p. 149).

[23] Wierzbicki, T. and Teng, X. (2003). "How the airplane wing cut through the exterior columns of the World Trade Center." *J. of Impact Engrg.* 28, pp. 601–625

[24] "World's tallest towers begin to show themselves on New York City skyline." *Engeering News Record*, 1/1/1970.

[25] Zeng, J.L., Tan, K.H., and Huang, Z.F. (2003). "Primary creep buckling of steel columns in fire." *J. of Construction Steel Research* 59, 951–970.

List of Figures

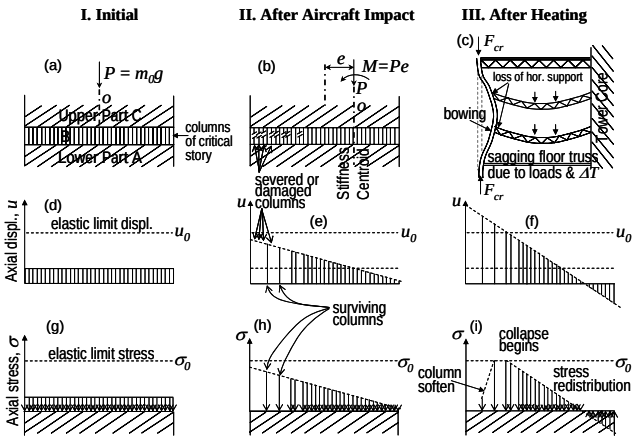
I. Initial
II. After Aircraft Impact
III. After Heating
(a)
$P = m_0 g$
Upper Part C
Lower Part A
columns of critical story
(b)
e
$M=Pe$
P
severed or damaged columns
Stiffness Centroid
(c)
F_{cr}
loss of hor. support
bowing
sagging floor truss due to loads & ΔT
Lower Part A
F_{cr}
(d)
Axial displ., u
elastic limit displ.
u_0
(e)
u
u_0
surviving columns
(f)
u
u_0
(g)
Axial stress, σ
elastic limit stress
σ_0
(h)
σ
σ_0
(i)
σ
collapse begins
column soften
stress redistribution
σ_0

Fig. 1

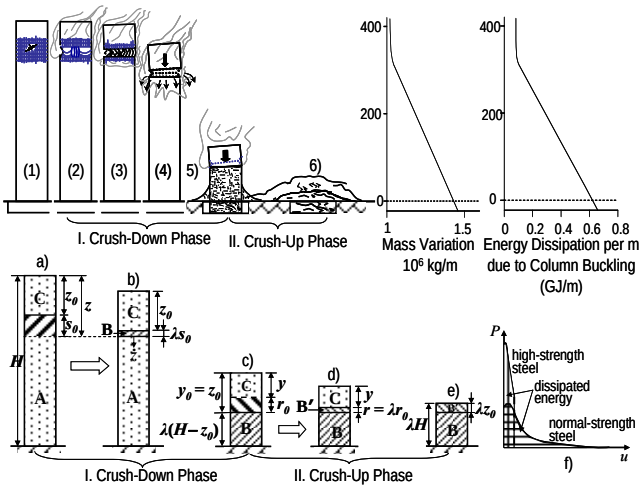
(1)
(2)
(3)
(4)
5)
6)
I. Crush-Down Phase
II. Crush-Up Phase
400
200
0
1
1.5
Mass Variation
10⁶ kg/m
400
200
0
0
0.2
0.4
0.6
0.8
Energy Dissipation per m
due to Column Buckling
(GJ/m)
a)
b)
c)
d)
e)
f)
C
A
B
B′
H
high-strength
steel
dissipated
energy
normal-strength
steel
P
u
I. Crush-Down Phase
II. Crush-Up Phase

Fig. 2

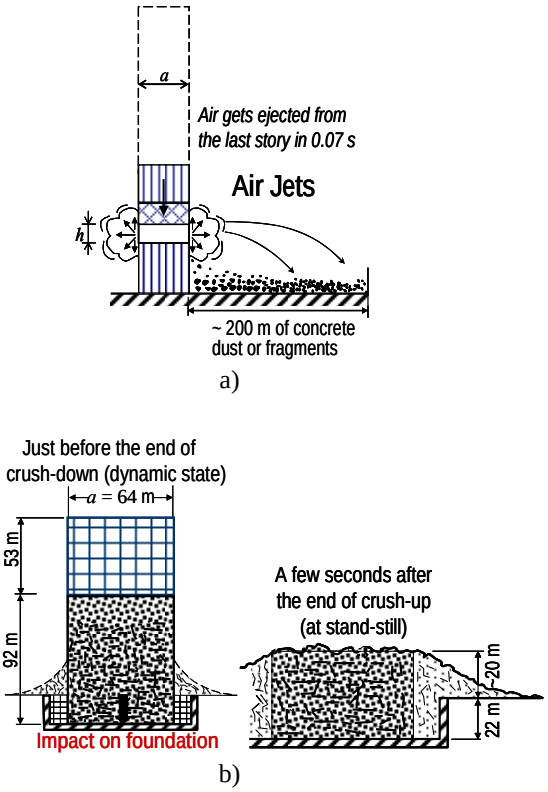
a
Air gets ejected from
the last story in 0.07 s
Air Jets
h
~ 200 m of concrete
dust or fragments
a)
Just before the end of
crush-down (dynamic state)
a = 64 m
53 m
92 m
Impact on foundation
A few seconds after
the end of crush-up
(at stand-still)
20 m
22 m
b)

Fig. 3

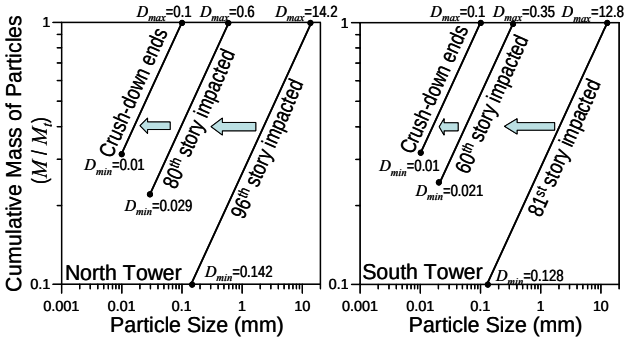
Cumulative Mass of Particles (M / M0)
Particle Size (mm)
Crush-down ends
80th story impacted
96th story impacted
North Tower
South Tower
60th story impacted
81st story impacted

a)

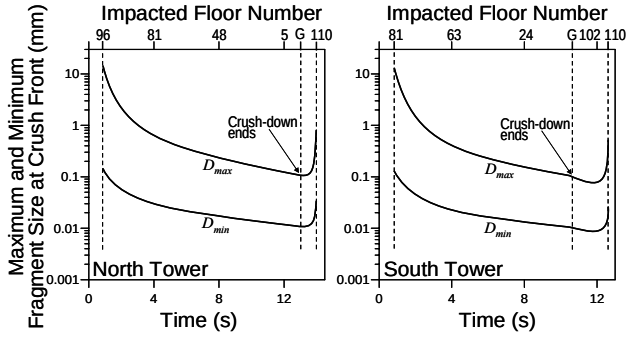
Impacted Floor Number
Maximum and Minimum Fragment Size at Crush Front (mm)
Time (s)
Crush-down ends
North Tower
South Tower

b)

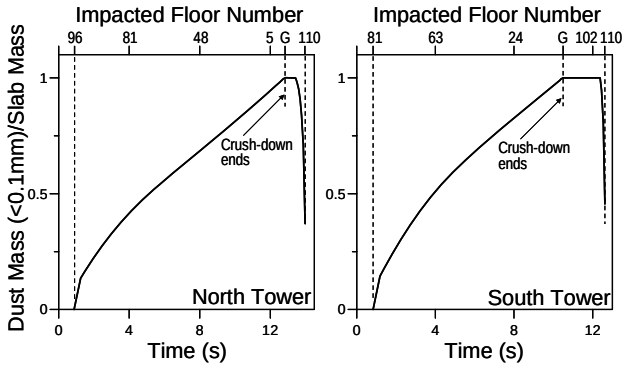
Impacted Floor Number
Dust Mass (<0.1mm)/Slab Mass
Time (s)
Crush-down ends
North Tower
South Tower

c)

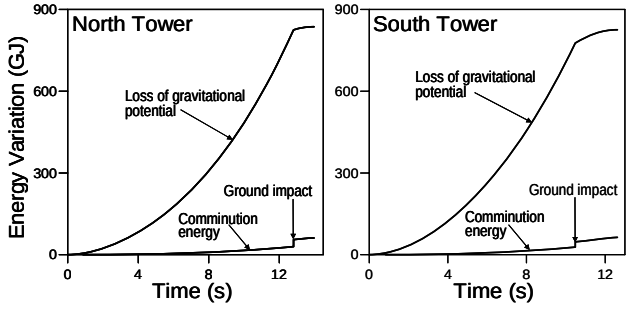
Energy Variation (GJ)
Time (s)
North Tower
South Tower
Loss of gravitational potential
Ground impact
Comminution energy

d)

Fig. 4

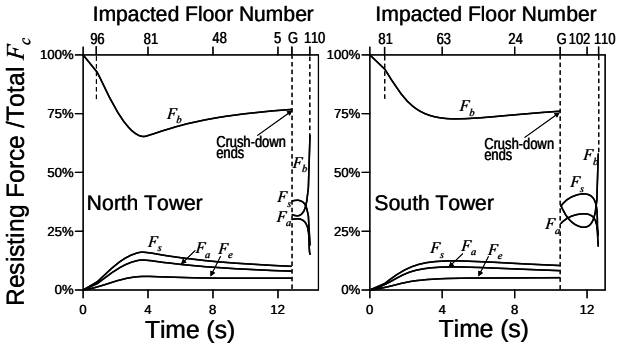
Impacted Floor Number
96 81 48 5 G 110
81 63 24 G 102 110
Resisting Force /Total F_c
100%
75%
50%
25%
0%
F_b
Crush-down ends
North Tower
South Tower
F_s
F_a
F_e
0 4 8 12
Time (s)

a)

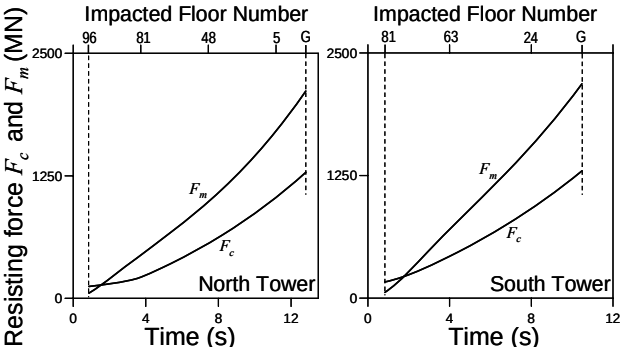
Impacted Floor Number
96 81 48 5 G
81 63 24 G
Resisting force F_c and F_m (MN)
2500
1250
0
F_m
F_c
North Tower
South Tower
0 4 8 12
Time (s)

b)

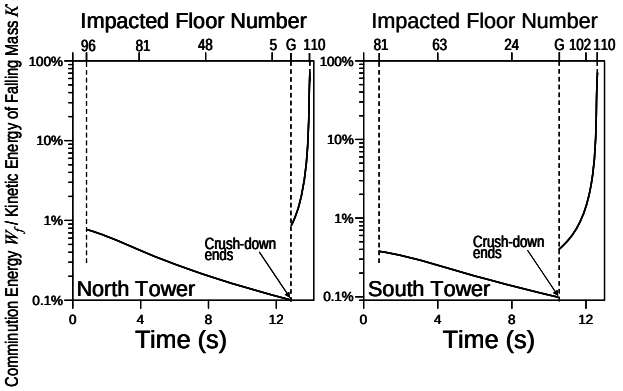
Impacted Floor Number
96 81 48 5 G 110
81 63 24 G 102 110
Comminution Energy W_f / Kinetic Energy of Falling Mass K
100%
10%
1%
0.1%
Crush-down ends
North Tower
South Tower
0 4 8 12
Time (s)

c)

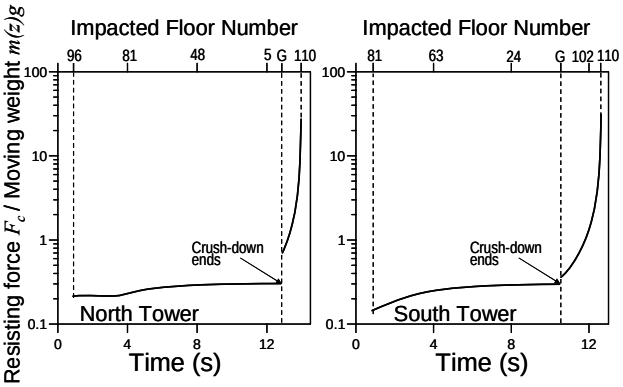
Impacted Floor Number
96 81 48 5 G 110
81 63 24 G 102 110
Resisting force F_c / Moving weight $m(z)g$
100
10
1
0.1
Crush-down ends
North Tower
South Tower
0 4 8 12
Time (s)

d)

Fig. 5

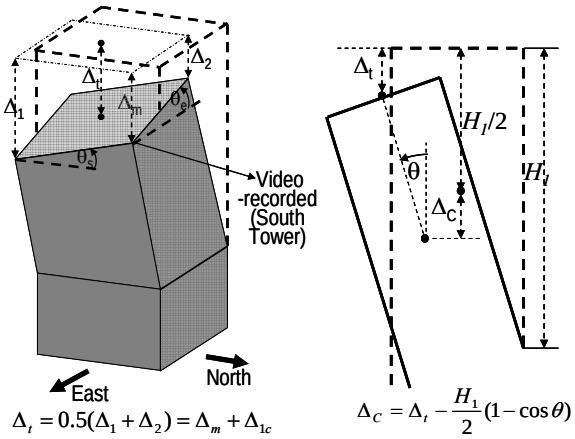
Δ1
Δ2
Δt
Δm
θ1
θ2
Video
-recorded
(South
Tower)
East
North
Δt = 0.5(Δ1 + Δ2) = Δm + Δ1c
Δt
H1/2
θ
H1
Δc
ΔC = Δt − H1/2 (1 − cos θ)
a)
Like a
tree?
No !
No !
Mass
Centroid
b)
c)
d)
e)

Fig. 6

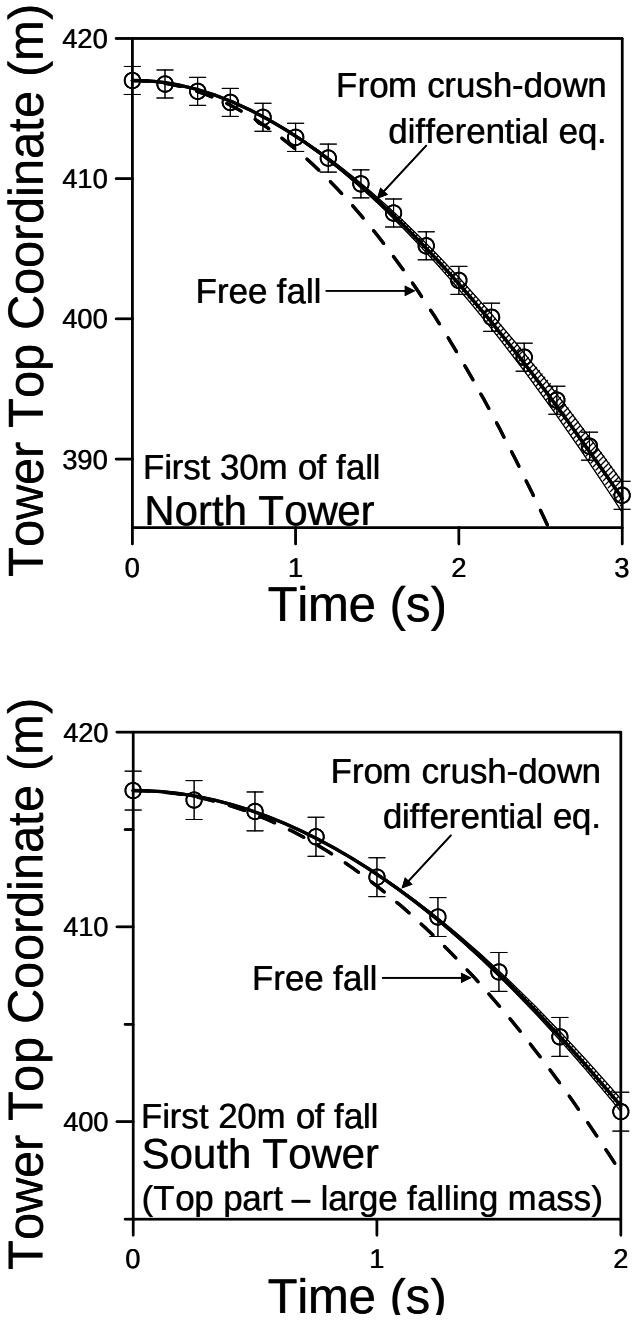
Tower Top Coordinate (m)
420
410
400
390
From crush-down
differential eq.
Free fall
First 30m of fall
North Tower
0
1
2
3
Time (s)
Tower Top Coordinate (m)
420
410
400
From crush-down
differential eq.
Free fall
First 20m of fall
South Tower
(Top part – large falling mass)
0
1
2
Time (s)

Fig.7

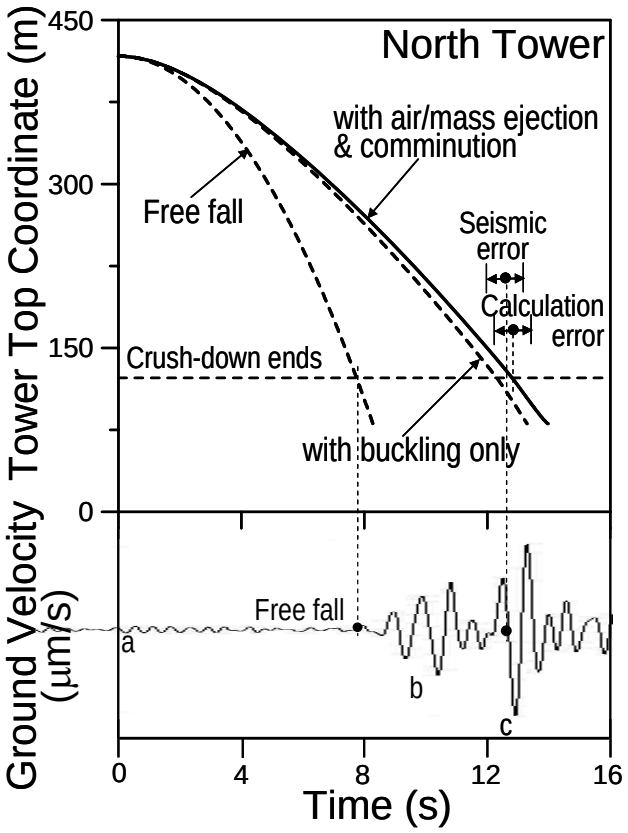
North Tower
with air/mass ejection
& comminution
Free fall
Seismic
error
Calculation
error
Crush-down ends
with buckling only
Free fall
a
b
c
Ground Velocity (μm/s)
Tower Top Coordinate (m)
Time (s)
450
300
150
0
0
4
8
12
16

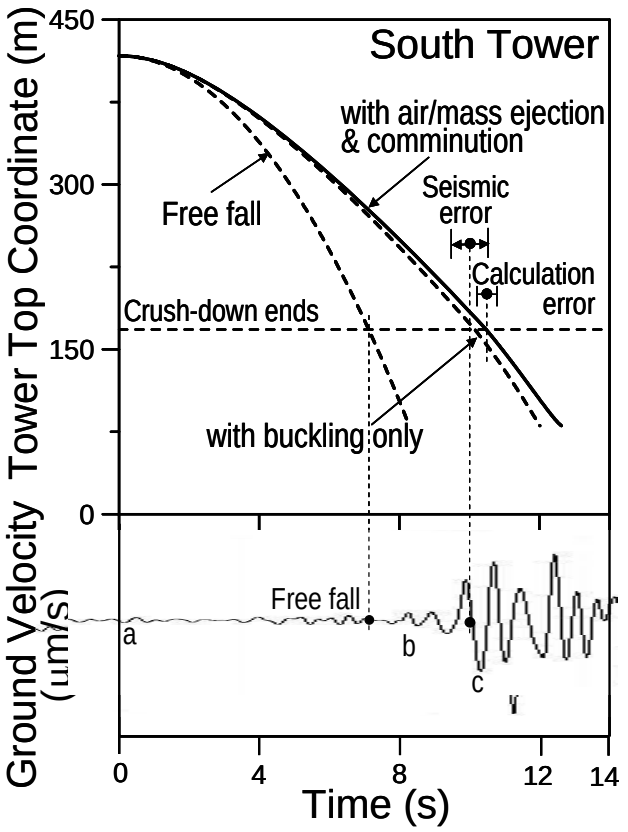
South Tower
with air/mass ejection
& comminution
Free fall
Seismic
error
Calculation
error
Crush-down ends
with buckling only
Free fall
a
b
c
Ground Velocity (μm/s)
Tower Top Coordinate (m)
Time (s)
450
300
150
0
0
4
8
12
14

Fig. 8

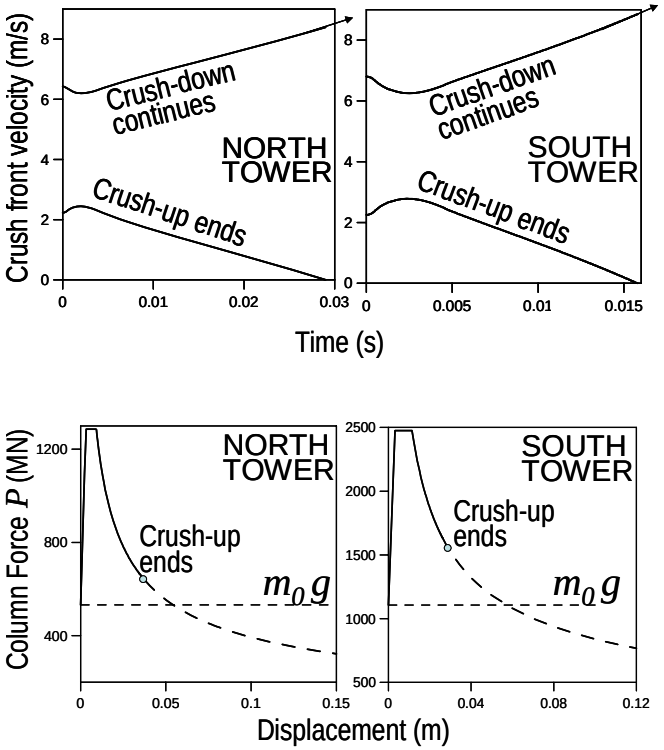
Crush front velocity (m/s)
Crush-down continues
NORTH TOWER
Crush-up ends
Crush-down continues
SOUTH TOWER
Crush-up ends
Time (s)
Column Force P (MN)
NORTH TOWER
Crush-up ends
$m_0 g$
SOUTH TOWER
Crush-up ends
$m_0 g$
Displacement (m)

Fig. 9